Investigation of Mutual Inductive Coupling in RF Stacked-Die Assemblies

Robert C. Frye, Kai Liu*, Haijing Cao†, Phoo Hlaing† and M. Pandi Chelvam†

RF Design Consulting, LLC
334 B Carlton Avenue
Piscataway, NJ 0885 USA
Tel: 908 217 5999
bob@RFDesignConsulting.com

*STATS ChipPAC, Inc.
1711 West Greentree, Suite 117
Tempe, Arizona 85284, USA
Tel: 480 222 1700
kai.liu@statschippac.com

† STATS ChipPAC, Ltd
5 Yishun Street 23
Singapore 768442
Tel: 65-6824-7888

Abstract

3D packaging is extensively used in digital applications, and is under consideration for analog RF applications as well. A key problem, however, is the coupling of strong output signals from front-end passive devices into the local oscillator of a transceiver chip. The main mechanism for this is mutual inductive coupling. In this study, a test structure has been designed, built and measured to examine the problem of mutual inductive coupling in stacked-die assemblies. Simulated results show good agreement with measurement, and can be used to predict the coupling. Additional simulation results are used to devise rough placement guidelines for the assembly to avoid excessive coupling. Surprisingly, even for modest amounts of lateral offset between coils on a stacked passive die and the tank coil of the underlying local oscillator, acceptably low levels of coupling can usually be obtained.

Introduction

Among the many method that have been proposed and implemented for 3D packaging [1] stacked chips with wire-bond connections to a common package is one of the simplest and most widely used. From its inception [2] applications of this technology have mainly been for digital memory because the digital bus architecture lends itself to highly parallel connections. Furthermore, the binary signal levels in digital circuits are generally large and robust, so coupled interference between the ICs is not a concern.

The general trend in packaging for RF wireless products, especially for consumer applications, is to reduce form-factor. This is leading to the adoption of 3-D packaging technology in wireless transceiver chips. Thin-film (e.g silicon-based) Integrated Passive Devices (IPDs) have form-factors that are ideally suited for stacked-chip assembly along with active RF transceiver ICs [3,4]. This poses some design challenges, however, because in comparison to digital applications, the analog signal levels in wireless systems are smaller, and even low levels of crosstalk between key functional blocks may significantly degrade the system performance.

Most common applications of IPDs are in the front-end of wireless systems, between the antenna and transceiver. These components need to meet stringent loss requirements, and consequently are too large to be practically integrated in RFICs. Matching balun transformers for power amplifiers are a typical example of such components [5]. As the use of multi-band transceiver chips becomes more common, significant board footprint reduction can be realized by integrating these components inside a common package with the transceiver.

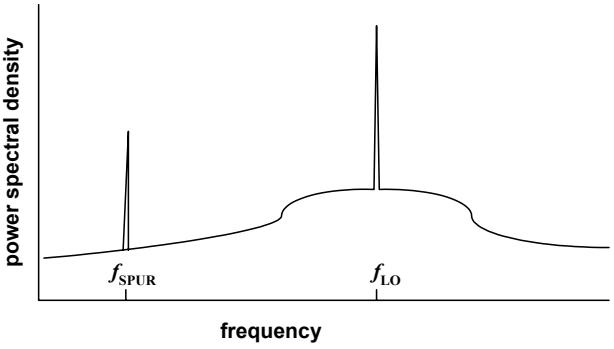

Figure 1: Local oscillator power spectral density.

LO Interference

A key concern in stacked die assemblies is that the strong output signal in the transmitter section of the RFIC may couple to the local oscillator (LO). The effect of this kind of interference on the local oscillator spectrum is sketched in Figure 1. The local oscillator in nearly all modern RFICs is composed of a voltage-controlled oscillator (VCO) that is synchronized to an external crystal reference through a phase-locked loop. This provides an on-chip oscillator of exceptional spectral purity. The local oscillator's frequency is usually offset from the transmit and receive frequencies to help avoid problems of interference.

The VCO itself typically consists of a cross-coupled amplifier circuit with a tuned resonant LC load. The inductor for this resonator is usually made up of one or two spiral inductor coils on the RFIC. The most straightforward mechanism for external signals coupling to the VCO is by magnetic induction directly into this resonator. If the external source is a periodic or quasi-periodic signal, it will introduce a spurious tone, indicated by f_{SPUR} in Figure 1.

In subsequent mixing, the RF signal is multiplied by the local oscillator signal to transpose the band of interest down

to low frequency for processing. The presence of a spurious tone in the local oscillator will cause out-of-band signals to be unintentionally mixed into the base-band frequency range. This degrades the receiver's sensitivity, adding both noise and crosstalk to the received signal.

In the design of stacked die assemblies incorporating RF transceivers, there is little that can be done to the circuit design to mitigate this kind of unwanted interference. Reducing the coupling to acceptable levels is mainly achieved by physical separation. However, there has been little investigation of the severity of the coupling or the amount of separation required, and there are no guidelines for these types of designs. The purpose of this study is to examine this issue and to develop some initial guidelines for the design of stacked die assemblies in RF applications.

Mutual Coupling Test Structure

The layout of a test structure designed to experimentally investigate the characteristics and the severity of inductive coupling in stacked-die assemblies is shown in Figure 2. In this structure, a two-turn inductor with ground-signal-ground probe pads is fabricated on the upper die of a two-die stack. The outer diameter of this inductor is 550µm. This size was chosen because it is typical of size of inductors used in IPD circuits.

The lower die has a series of small, single-turn inductors with similar probe pads, and a diameter of 200µm. These small inductors are spaced at regular 250µm intervals. Their size is typical of inductors used in the tank resonators of local oscillators in RF transceiver ICs. The purpose of these lower coils is to probe the strength of the mutual inductive coupling between the upper and lower die as a function of lateral offset. By using typical sizes, the overall flux linkage into the test coil is about the same as in an actual stacked die application.

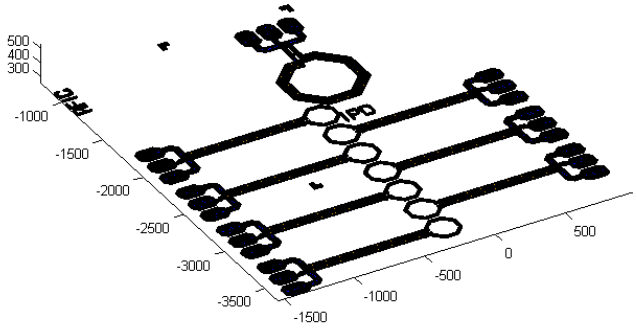

Figure 2: Layout of the stacked die test structure.

A micrograph of the assembled test structures is shown in Figure 3. Two types of testers, with and without ground shields, were evaluated. In the shielded structure, shown on the right, a coplanar ground shield covers the area surrounding the coil of the upper die. The coplanar shield has an opening in it to accommodate the coil.

In all of the devices tested, the thickness of the both the upper and lower die in the final assembly was 250µm. The stacked die was attached using non-conductive epoxy.

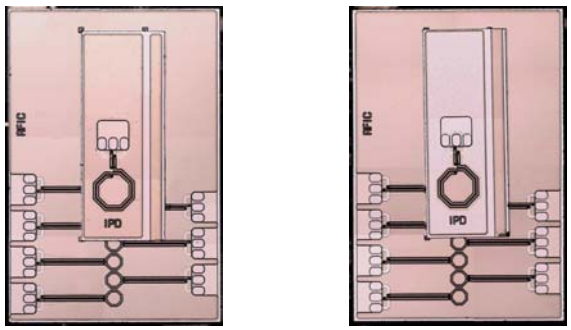

Figure 3: Micrographs of the assembled stacked die test structures without (left) and with (right) a ground shield surrounding the upper coil.

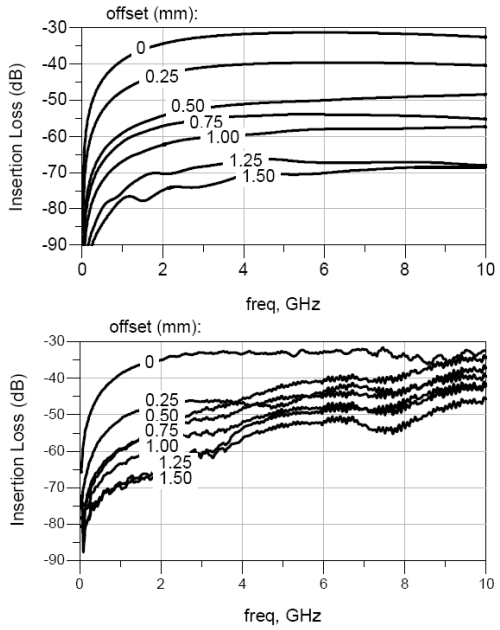

Figure 4: Comparison of simulated and measured insertion loss for the test structure without ground shield.

Experimental Results

The coupling between the top inductor coil and each of the lower probe coils was measured by vector network analyzer from 10MHz to 10GHz. A comparison of the raw measured insertion loss with simulation is shown in Figure 4. Here, it can be seen that the results are in general agreement up to about 3GHz. Above this frequency the measured results are degraded by imperfect isolation between the input and output probes. In general the measured insertion loss is high, and the level of signal transmitted between the two ports is very low. For the larger values of offset, with insertion loss in the 60 to 80dB range, the imperfect isolation limits the ability

to resolve these small signals. Even the simulation shows evidence of numerical noise at the lowest levels.

The coupling measurements are further influenced by the presence of the probes themselves, since these are large enough to distort the magnetic fields in the neighborhood of the coils. For purposes of analysis, the S-parameter results were evaluated in the range below 3GHz, where agreement between measurement and simulation is reasonably good. Overall, especially at higher frequencies, the simulated results are probably a better indicator of the reality of the situation than the measurements because of the experimental difficulties inherent in this structure.

In the general problem of coupling between inductor coils, we are not so concerned with S-parameters (which are the measured observable quantity) but rather with the coupling coefficient between the coils. This can be extracted from the two port inductance matrix for this circuit. To derive this, the S-parameters are first converted to Z-parameters, and then the inductance matrix is defined as

$$L_{ij} = imag(Z_{ij}) / (2\pi f) \tag{1}$$

The coupling coefficient is then given by

$$k = L_{12} / \sqrt{L_{11} L_{22}} \ . \tag{2}$$

At frequencies well below the inductors' self resonances, the inductance and coupling coefficient are more or less independent of frequency. Figure 5 shows both measured and simulated coupling coefficient versus lateral offset for the test structure. These results were evaluated at 2.5GHz, but are roughly independent of frequency from dc to 4GHz. It is not apparent from the plots of the measured results, which are shown on a logarithmic scale, but there is a sign reversal in the coupling that occurs at some point between 0.25 and 0.5mm lateral offset.

Also shown in Figure 5 is an analytical result. The z-axis component of the magnetic field from a circular loop of current can be calculated analytically [6], and used to estimate the flux linkage through a smaller loop at a given vertical and lateral offset. This analytical result is only approximate, since it assumes infinitesimal conductor thickness and vanishingly small loop area in the lower die. It is useful, however, because it helps to illustrate the general nature of the coupling. Like the measured results, it shows a null in the coupling with a sign reversal at larger offsets. This null occurs at a distance that is comparable to, and somewhat larger than the sum of the radii of the two coils. It roughly corresponds to the separation at which the two coils, viewed from above, do not overlap.

Figure 6 shows a sketch of the magnetic field lines surrounding the coil that helps to explain the reason for the sign reversal. In the region inside the windings of the coil on the IPD, the field lines are oriented downward into the top surface of the RFIC. Mutual inductive coupling is proportional to the flux linkage into the coil on the RFIC, so it depends only on the z-axis component of the field. In the region far to the right, the field lines re-emerge from the RFIC, and the sign of the flux linkage is reversed. At some intermediate point the field lines are exactly tangential to the RFIC surface, and there is a null in the flux linkage.

Figure 7 compares the coupling with and without a coplanar ground shield on the upper die. In a coplanar structure, the regions outside the components and interconnections are filled with a ground plane. Because it is necessary to open holes and to provide clearance between the circuits and ground, coplanar ground is less effective than a microstrip structure having a solid ground plane. However, in thin-film technologies the thickness of the dielectrics is not sufficient to allow the use of such a ground plane.

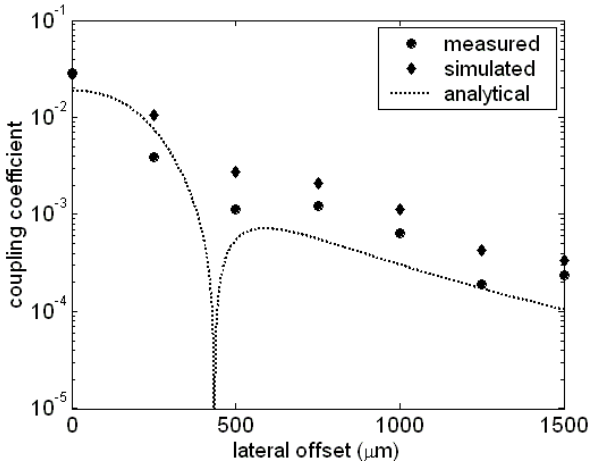

Figure 5: Coupling coefficient versus lateral offset for the stacked die test structure.

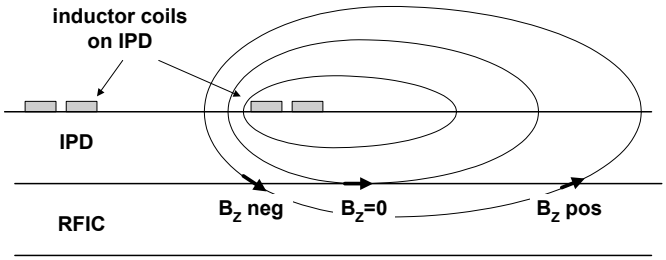

Figure 6: Magnetic field lines surrounding an inductor coil, showing the sign reversal in the vertical component.

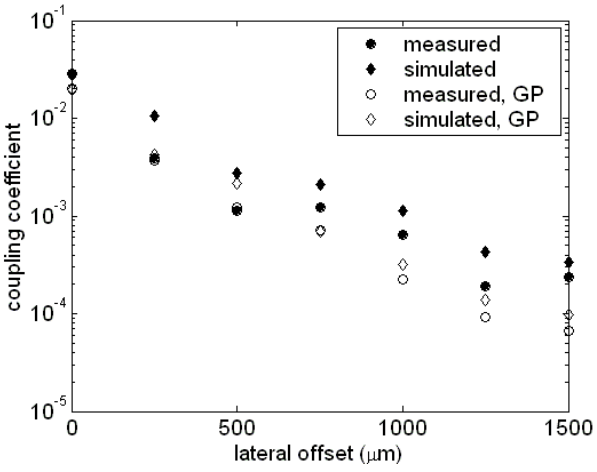

Figure 7: Comparison of coupling with (open markers) and without (solid markers) a coplanar ground shield.

Consequently, coplanar grounds are more commonly used in such cases, or more commonly the devices are left unshielded.

In all cases, the measured value of coupling coefficient is smaller than simulated. This reflects the same problems of isolation that affected the raw S-parameters. The RF probes themselves are physically large, and introduce some degree of additional coupling to the devices that are being tested. Coupling of this nature cannot be compensated for during calibration, and is an inherent source of error in measurements like this. Note that at zero offset, where the coupling between the coils is strongest, measurement and simulation are in very close agreement.

It can be seen in Figure 7 that for small values of lateral offset, i.e. in the regions beneath the upper inductor, there is little difference between shielded and unshielded structures. At larger values of offset, the coupling in the shielded structure falls off more steeply. Examination of these two cases on a log-log scale shows that the tails of the coupling response for the unshielded case fall off as the square of the distance, and for the shielded case as the cube. However, over the distance shown – up to a maximum offset of 1.5mm – the effect of the shield is only modest. Coplanar ground shields are mainly effective in eliminating far-field coupling. The amount of offset that can be obtained within the size constraints of a typical RFIC – one or two millimeters at most – limits the improvement that can be obtained from the shield. For practical values of offset, the coplanar ground shield reduced the coupling by a factor of 2 to 4.

Extension to General Problems

In general, for two coupled inductors

$$v_1 = j\omega L_{11} i_1 + j\omega L_{12} i_2 \text{ and } v_2 = j\omega L_{12} i_1 + j\omega L_{22} i_2 , \qquad (3)$$

where the elements of the inductance matrix, L_{ij}, are as described above. It is assumed that v_1 is the voltage across the LO inductor and v_2 is the voltage across the interfering IPD inductor. If the coupling is small, then for the IPD inductor the voltage and current are approximately related by

$$v_2 \approx j\omega L_{22} i_2 \qquad (4)$$

and the voltage on the LO inductor can be written as

$$v_1 \approx j\omega L_{11} i_1 + k\sqrt{\frac{L_{11}}{L_{22}}} v_2 . \qquad (5)$$

In (5), the first term on the right hand side represents the LO signal (presumably large), and the second term is the interference that is introduced by the IPD (presumably much smaller). The interference voltage on the LO coil is related to the voltage on the IPD coil by

$$v_{INT} = k\sqrt{\frac{L_{11}}{L_{22}}} v_{IPD} \qquad (6)$$

So the height of the spur in the power spectrum, as shown in Figure 1, is related to the height of the main signal by

$$PSD_{SPUR}(dBc) = 20\log_{10}\left[k\sqrt{\frac{L_{11}}{L_{22}}} \frac{v_{IPD}}{v_{LO}} \right]. \qquad (7)$$

In (7), v_{LO} is the amplitude of the signal oscillation voltage on the LO coil. The spur amplitude is measured in dBc, where the zero reference is the signal amplitude (i.e. the main peak is at 0 dBc).

In most cases (and especially on a dB scale) the inductance of the IPD inductor, L_{22}, and of the LO inductor, L_{11}, are comparable, as are the amplitudes of the voltages across them. So, to a rough approximation

$$PSD_{SPUR}(dBc) \approx 20\log_{10}(k) . \qquad (8)$$

Without being specific about the conditions of loading on the coils or the drive conditions, Equation 8 can be used to estimate the level of interference. This is useful early in the design.

In the measured test structures, for example, the coupling coefficient at a lateral offset of 0.5mm is about $3 \cdot 10^{-3}$, giving an estimated PSD for the spur of -50.5dBc. This is a surprisingly low level of interference given the proximity of the components, and would not significantly degrade the system performance in most applications.

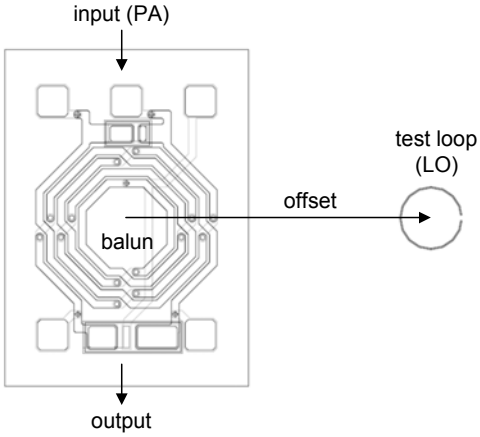

Figure 8: Configuration for analyzing coupling between a PA balun and the LO inductor.

Design Examples

The measured characteristics of the stacked die tester demonstrate the general characteristics of mutual inductive coupling and validate the accuracy of electromagnetic simulations for characterizing the levels of interference. However, most circuit applications of IPDs in RF transceivers are significantly more complex than simple inductors. In this section, some representative examples of front-end circuits are analyzed.

A common example of a front-end circuit that would be used in a stacked-die assembly is a coupled inductor balun. These are often used to convert the differential output signal from a power amplifier (PA) into a single-ended signal. Additionally, such circuits can also act as matching networks

to transform the complex output impedance of the PA into a standard real impedance, like 50Ω. The simulation setup for an example balun design is shown in Figure 8.

The coupled inductor balun consists of two concentric, nested spiral inductors with resonating capacitors. In operation, signals passing through the balun cause currents to flow in the opposite direction on the two inductors. So, while the external fields are similar to those in a simple inductor, the magnetic fields in the two coils partially cancel.

The example balun shown in Figure 8 is a DCS balun designed to operate from 1710 to 1910MHz. The test loop representing the LO is also shown in the drawing. This loop is a single-turn with a diameter of 200µm. For these simulations, the lateral offset is measured from the center of the balun, as shown in the figure.

The results of the simulation are shown in Figure 9. The upper curve shows the calculated LO coupling into the output (which is not usually of much concern). The lower curve shows the coupling of the power amplifier output signal back into the LO. This shows qualitative behavior very similar to that of a simple inductor. Resistive losses and capacitive coupling in the circuit damp the null, so that it never really passes through zero, but the dip in the coupling arises from the same mechanism that produced a complete null in the ideal analytical case. Note that the coupling in the region to the right of the null is lower than for a simple inductor of comparable size. This is a result of the partial cancellation in the magnetic fields from the two sides of the coupled inductor.

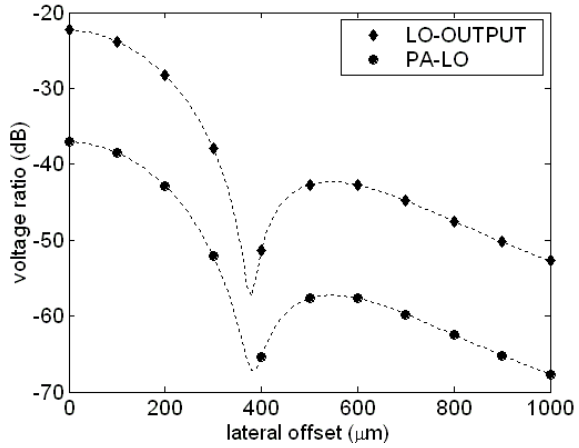

Figure 9: Calculated voltage coupling for a DCS balun at 1850MHz.

In an actual application, the test loop shown in Figure 8 would be replaced by the actual layout of the inductor in the LO. In addition, the loading on the inductor (typically a resonating capacitor) would also be included in the simulation. In general, the coupling into the test loop will be proportional to the flux linkage, so it will scale with the number of turns and the loop area. Overall, these considerations will change the result by a few dB. The surprising and useful result of the calculation, however, is that for reasonable amounts of lateral offset between the balun coil and the underlying LO resonator, the coupling from the PA output into the LO can be kept to an acceptably low level for

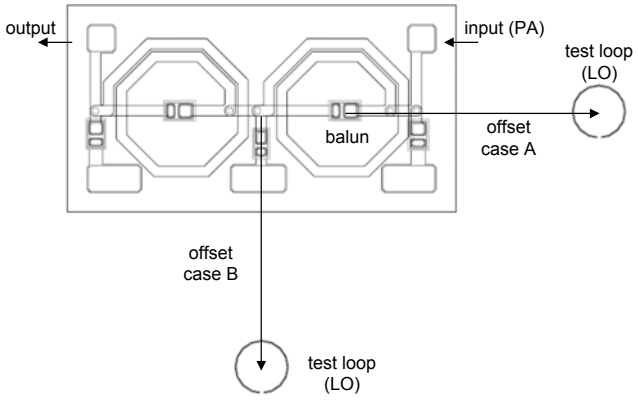

Figure 10: Layout for coupling simulation for a DCS low-pass filter. Two cases for lateral offset are shown.

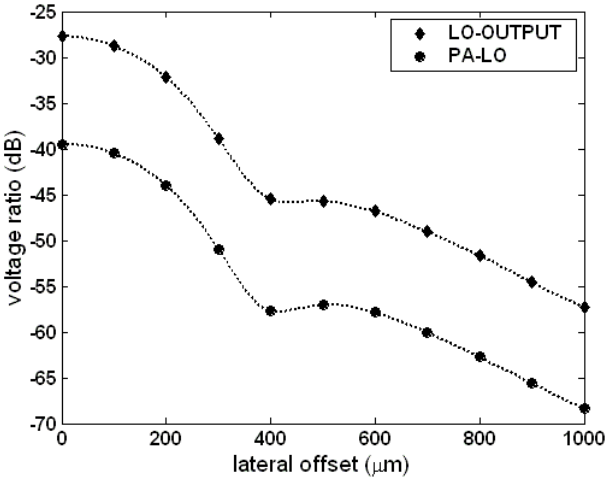

Figure 11: Calculated voltage coupling for a DCS low-pass filter at 1850MHz, Case A.

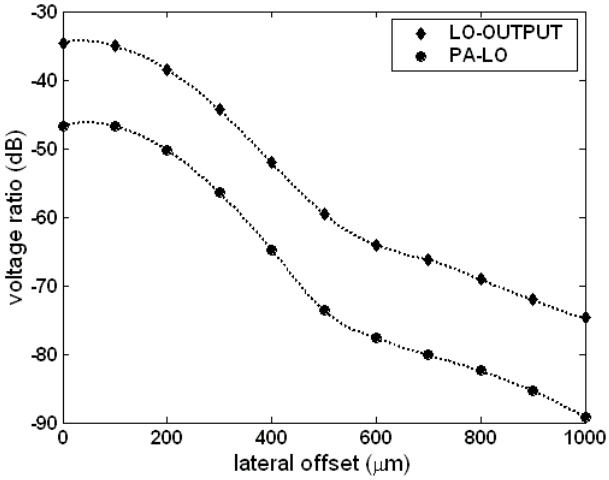

Figure 12: Calculated voltage coupling for a DCS low-pass filter at 1850MHz, Case B.

most applications.

A second common IPD circuit type is shown in Figure 10. This circuit is a low-pass filter. Low pass filters are often used to eliminate harmonics from the output of power amplifiers. The filter in this particular example is a 5-pole elliptic design with two inductors. Two different cases are considered: In case A the offset between the filter and the underlying LO is along the axis of the filter starting from the center of one of the inductors, and in case B it is normal to the filter axis, starting from the filter center. These two cases look not only at the effects of separation, but also of orientation.

Simulated coupling results for Case A are shown in Figure 11. These are similar to the balun results, except that the depth of the null is greatly reduced. This is mainly a consequence of having two coils. At most locations in the x-y plane the null field regions in the two coils do not coincide. However, the overall levels of coupling are similar to those of a simple inductor, and it can be seen by comparison with Figure 9 that the coupling is quite similar to the balun example.

The simulated coupling for Case B is shown in Figure 12. By comparison, it can be seen that the overall level of coupling is smaller by 8dB at small offsets and as much as 20dB at large offset. This is because the offset axis in Case B lies along an axis of symmetry in the circuit. The current flowing in both of the filter coils is similar, and their fields tend to cancel along this axis. It is sometimes the case, especially in differential circuits, that such axes can be identified and used to advantage in determining the best placement of stacked die.

Conclusions and Guidelines

Clearly, coupling is strongest when coils on two levels of stacked die are placed directly one atop the other. For the 250µm thick IPD used in this study, this results in coupling at the -30 to -40dBc level. For thinner die it would be even stronger. Similar levels of coupling occur for lateral offset that results in any significant overlap of the coils. So, if possible, the IPD should be placed such that no part of the IPD coil or coils overlaps any part of the LO coil on the RFIC.

Beyond this region of overlap and strongest coupling, the coupling falls rapidly to generally acceptable levels for most applications. In unshielded IPDs the tails of the coupling fall off roughly with the square of the distance. In this zone, for reasonable values of lateral offset in the 0.5mm or more, the coupling will be in the -50dBc or lower range. This is adequate isolation for most applications and is usually not a difficult amount of separation to achieve.

Coplanar ground shields cause the coupling in the far field to fall off more rapidly, roughly with the cube of the distance. This difference in response only becomes significant for lateral offset of 1mm or more, however. In most practical cases it does not make enough difference to merit the added design difficulties that accompany a coplanar shield. Shielding may prove useful in more demanding applications, especially those that are marginal for an unshielded design. In such cases, the added improvement from the ground shield may be worthwhile.

The results of this investigation are encouraging for the feasibility of stacked die assemblies in RF applications. With moderate care to ensure that the coils in IPD circuits do not overlap the main tank resonator in the RFIC's local oscillator, remarkably good isolation between the IPD and LO can be obtained.

Acknowledgment

The authors are grateful to Brett Dunlop help in initiating this investigation.

References

1: S. F. Al-Sarawi, D. Abbott and P. D. Franzon, "A Review of 3-D Packaging Technology," IEEE Trans. Components, Packaging and Manuf. Tech. B-21, 1, pp. 2-14 (1998)

2: D. B. Tuckerman, L.-O. Bauer, N. E. Brathwaite, J. Demmin, K. Flatow, R. Hsu, P. Kim, C.-M. Lin, K. Lin, S. Nguyen, and V. Thipphavong, "Laminated memory: A new 3-dimensional packaging technology for MCM's," Proc. 1994 IEEE Multi-Chip Module Conf. MCMC-94, 58–63, Santa Cruz, CA, Mar. 1994

3: K. Liu and R. C. Frye, "Small Form-Factor Integrated Passive Devices for SiP Applications," Proc. IEEE MTT-S Int'l. Microwave Symposium, 2117-2120 Honolulu, June 5-7, 2007

4: R. C. Frye, Y. Lin, G. Badakere, B. Dunlap and E. Gongora, "The Impact of SiP Performance and Form-Factor Requirements on IPD Technology," Proc. IMAPS 36th Int'l. Symposium on Microelectronics, 590-595 San Diego, Oct 8-12, 2006

5: R. C. Frye, G. Badakere, Y. Lin and M. P. Chelvam, "A Monolithic, Compact Balun/Matching Network for SiP Applications," Proc. IEEE 13th Topical Meeting on Electrical Performance of Electronic Packaging, 37-40 Portland, Oct 25-27, 2004

6: W.R. Smythe Static and Dynamic Electricity, p. 266, McGraw-Hill, New York, 1950.